J Membrane Biol (2010) 237:125–136
DOI 10.1007/s00232-010-9314-x

Formation of Macromolecule Complex with *Bacillus thuringiensis* Cry1A Toxins and Chlorophyllide Binding 252-kDa Lipocalin-Like Protein Locating on *Bombyx mori* Midgut Membrane

Ganesh N. Pandian · Toshiki Ishikawa · Thangavel Vaijayanthi · Delwar M. Hossain · Shuhei Yamamoto · Tadayuki Nishiumi · Chanan Angsuthanasombat · Kohsuke Haginoya · Toshiaki Mitsui · Hidetaka Hori

Received: 24 May 2010 / Accepted: 26 October 2010 / Published online: 16 November 2010

Abstract P252, a 252-kDa *Bombyx mori* protein located on the larval midgut membrane, has been shown to bind strongly with *Bacillus thuringiensis* Cry1A toxins (Hossain et al. Appl Environ Microbiol 70:4604–4612, 2004). P252 was also shown to bind chlorophyllide (Chlide) to form red fluorescence–emitting complex Bm252RFP with significant antimicrobial activity (Pandian et al. Appl Environ Microbiol 74:1324–1331, 2008). In this article, we show that Cry1A toxin bound with Bm252RFP and Bm252RFP–Cry1A macrocomplex, with both antimicrobial and insecticidal activities, was formed. The insecticidal activity of Bm252RFP–Cry1Ab was reduced from an LD_{50} of 1.62 to 5.05 μg, but Bm252RFP–Cry1Aa and Bm252RFP–Cry1Ac did not show such reduction. On the other hand, the antimicrobial activity of Bm252RFP–Cry1Ab was shown to retain almost the same activity as Bm252RFP, while the other two complexes lost around 30% activity. The intensity of photo absorbance and fluorescence emission of Bm252RFP–Cry1Ab were significantly reduced compared to those of the other two complexes. Circular dichroism showed that the contents of Cry1Ab α-helix was significantly decreased in Bm252RFP–Cry1Ab but not in the other two toxins. These data suggested that the reduction of contents of α-helix in Cry1Ab affected the insecticidal activity of the macrocomplex but did not alter the antimicrobial moiety in the macrocomplex of Bm252RFP–Cry1Ab.

Keywords Antimicrobial activity · *Bacillus thuringiensis* Cry1A toxin · Chlorophyllide-binding protein · Insect midgut membrane · Insect immunity · Red fluorescent protein

G. N. Pandian · T. Ishikawa · T. Vaijayanthi · D. M. Hossain · S. Yamamoto · T. Nishiumi · K. Haginoya · T. Mitsui · H. Hori
Graduate School of Science and Technology, Niigata University, Niigata 950-2181, Japan

C. Angsuthanasombat
Institute of Molecular Biosciences, Mahidol University, Nakornpathom 73170, Thailand

H. Hori (✉)
Laboratories of Applied Biosciences, Graduate School of Science and Technology, Niigata University, Niigata 950-2181, Japan
e-mail: hide-hri@gs.niigata-u.ac.jp

Introduction

Bacillus thuringiensis (Bt) insecticidal Cry toxin is the most widely used biopesticide due to its narrow target specificity and safety toward other vertebrates and beneficial arthropods (Federici 2003; Kough 2003). Pore formation mediated by the binding of Cry toxins to receptors such as aminopeptidase N (Gill et al. 1995; Knight et al. 1994; Sangadala et al. 1994; Valaitis et al. 1995) or cadherin-like proteins (Vadlamudi et al. 1995; Ihara et al. 1998; Nagamatsu et al. 1998) in larval midgut epithelial cells is the tentative but widely accepted insecticidal mechanism (Schnepf et al. 1998; Pigott and Ellar 2007).

Despite their effectiveness for about 40 years, development of insect resistance to Bt toxins has threatened the sustained successful application of Bt formulation in biological control strategies (Ferré and Van Rie 2002; Bravo et al. 2007; Tabashnik 1994). The diamondback moth, *Plutella xylostella*, and the cabbage looper, *Trichoplusia ni*, are the popular species that have developed Bt resistance in

the open field (Janmaat and Myers 2003; Shelton et al. 1993).

Effective management of Bt-resistant insects requires a thorough understanding of the resistance mechanisms. Some plausible mechanisms for the resistance to Bt toxins have been reported, such as (1) altered binding of Bt toxins to midgut receptors, (2) changes in the activation or degradation of Bt toxins by digestive proteases and (3) changes in receptor conformation that interfere with toxin binding (Van Rie et al. 1990; Heckel 1994; Griffitts and Aroian 2005). Exploring Bt toxin receptors will provide new insight into the *Bt* toxin mode of action and the mechanism of Bt toxin resistance, which are not yet fully understood.

P252 is the midgut membrane protein of *Bombyx mori* larvae which binds to Bt toxins of Cry1Aa, Cry1Ab and Cry1Ac with K_d values of nanomolar order and was suggested as a possible receptor candidate involved in the insecticidal and/or resistance mechanisms (Hossain et al. 2004, 2005). We have recently shown that P252 is a chlorophyllide (Chlide)–binding protein forming a P252–Chlide complex, termed Bm252RFP. This complex exhibits red fluorescence as well as strong antimicrobial activity against *Escerichia coli*, *Serratia marcescens*, *Bt* and even *Saccharomyces cerevisiae* with relatively low activity (Pandian et al. 2008). Furthermore, three internal peptides of P252 were shown to have almost identical homology with lipocalin protein (Mauchamp et al. 2006; Pandian et al. 2008).

In this report, interestingly, we find that Bm252RFP bound with Cry1A and formed a macrocomplex of Bm252RFP–Cry1A. This complex showed insecticidal and antimicrobial activities, although the intensities were not the same as that of Cry1A and Bm252RFP, respectively. We also show the kinetics of the formation of Bm252RFP–Cry1A macrocomplex and evidenced about the different fashion of complex formation in Cry1Ab from that in the other two toxins. Although the physiological functions of those macrocomplexes in vivo are not elucidated, we briefly discuss the possibility of detoxification of Cry1Ab with the formation of Bm252RFP–Cry1Ab, which might contribute to an understanding of the roles of the insect midgut and of macrocomplexes in resistance.

Materials and Methods

Insect Larvae

The silkworm, *Bombyx mori*, hybrid strain Shunrei × Shogetsu, was reared on an artificial diet of Silkmate (Nosan Kogyo, Yokohama, Japan), and 1-day-old fifth-instar larvae were used in the following experiments.

Culture of Microbes and Production of Cry1A

To assess antimicrobial activity, *E. coli* JM109, *Se. marcescens* 2170, *Bt sotto* strain T84A1 and yeast, *Sa. cerevisiae* were cultured as described in Pandian et al. (2008).

Bt sotto strain T84A1, a gift from Dr. M. Ohba, and HD-73 were cultured for the production of Cry1Aa and Cry1Ac, respectively, in NYS medium (Suzuki et al. 1992). Cry1Ab was obtained from recombinant *E. coli* JM109 harboring pYD4.0 encoding the full-length *cry1Ab* gene (Kim et al. 1998). The insecticidal crystal proteins obtained were solubilized and activated with immobilized trypsin as described in Indrasith et al. (1991) and purified as described in Hossain et al. (2004) using ion exchange and gel filtration chromatography.

Preparation of P252 and Bm252RFP

P252 was purified from brush border membrane vesicles (BBMVs) of *B. mori* larvae using gel filtration and ion exchange chromatography as reported by Hossain et al. (2004). Chlide-A was purchased from Sigma-Aldrich (St. Louis, MO) and prepared from fresh spinach (Pandian et al. 2008). Bm252RFP was prepared by incubating 1 μM P252 with 50 μM Chlide under aerobic, light conditions at 6,000 μmol m^2/s (Pandian et al. 2008). In this condition, all Chlide is consumed to form Bm252RFP. Furthermore, SDS-PAGE showed that no protein was degraded from Bm252RFP.

Formation of Bm252RFP–Cry1A with Bm252RFP and Cry1A

Bm252RFP was incubated with each Cry1A toxin to form Bm252RFP–Cry1A. To study the concentration dependence of the macrocomplex formation, each Cry1A toxin was kept constant at 1.0 μM, and various concentration of Bm252RFP from 0.5 to 2.5 μM were incubated at 25°C for 1.5 h. Unreacted Cry1A were determined with Western blot analysis, as shown later. Binding between Bm252RFP and Cry1A toxins was further confirmed by size-exclusion liquid chromatography (model 2110; Bio-Rad, Richmond, CA) using a GPC-1000 column (for MW ranges 40–1000 kDa; Eprogen, Downers Grove, IL), and unreacted Cry1A toxins were separated from Bm252RFP–Cry1A and quantified with absorbance at 280 nm.

The optimum ratio between each Cry1A and Bm252RFP to form the macrocomplex was determined as 1:1.6, 1:2.2 and 1:1.6 for Bm252RFP–Cry1Aa, -Cry1Ab and -Cry1Ac, respectively. In this condition, almost all toxins were shown to bind to form Bm252RFP–Cry1A.

From this synthetic reaction, the dissociation constant of the binding between Bm252RFP and Cry1A was calculated using a Scatchard plot as modified by Coleman and Pugh (1997).

Determination of Bm252RFP and Bm252RFP–Cry1A Concentrations

Bm252RFP emits specific fluorescence at 620 nm, and this characteristic fluorescence was used to quantify the concentration of those macrocomplexes. In the case of Bm252RFP–Cry1Aa and –Cry1Ac, the specific fluorescence derived from Bm252RFP was not affected by the binding of Cry1A toxins. However, Bm252RFP–Cry1Ab significantly reduced its fluorescence, as shown in the results; therefore, the Bm252RFP–Cry1Ab concentration was briefly determined with Western Blotting using anti Cry1Aa antisera, as described later.

Determination of Various Parameters Affecting the Stability of Bm252RFP–Cry1A

The stability of Bm252RFP–Cry1A under various parameters was checked. Bm252RFP–Cry1A was incubated for 48 h in 20 mM Tris-HCl containing 50 mM NaCl under various different parameters, and their influence on stability was evaluated by measuring the released Cry1A using Western blot analysis and the released Chlide using TLC (Pandian et al. 2008). To evaluate the stability at various pH values, Bm252RFP–Cry1A was dissolved in 20 mM phosphate buffer for pH 6–7, 20 mM Tris-HCl buffer for pH 7–10 and 20 mM glycine-NaoH buffer for pH 10–11. Each buffer contained 50 mM NaCl. In addition, the stability of the macrocomplexes was determined under various temperatures and light intensities, as shown in the results. The conditions such as aerobic and anaerobic, each with or without light, were also employed as described in Pandian et al. (2008).

Bioassay of Bm252RFP–Cry1A Antimicrobial Activity

Cultures of *Se. marcescens* 2170, *E. coli* JM109, *Bt sotto* TA81 and *Sa. cerevisiae* were grown; and the cell concentration of the cultures was adjusted as previously described (Pandian et al. 2008).

Bm252RFP–Cry1A was synthesized by incubating Bm252RFP and individual Cry1A as described above. Regardless of the optimized ratio between Cry1A and Bm252RFP for the complex formation (Cry1A:Bm252RFP = 1:1.5–2.3), Cry1A was employed with a two times higher ratio to avoid the occurrence of unreacted Bm252RFP that could influence antimicrobial activity.

After appropriate dilution, each microbial culture was incubated with the synthesized macrocomplex at various concentrations for 4 h at 37°C for bacteria or at 30°C for yeast. Colony-forming units (CFUs) per milliliter were counted to obtain the 50% effective concentration (EC_{50}) as described in Bergman et al. (2006) and in Pandian et al. (2008).

Cry1A did not have antimicrobial activity; thus, when we calculated the activity, the molar concentration of Bm252RFP–Cry1A was expressed as that of only Bm252RFP. Thus, a direct comparison of the change in specific antimicrobial activity of Bm252RFP on the formation of Bm252RFP–Cry1A was possible.

Bioassay of Bm252RFP–Cry1A Insecticidal Activity

For the bioassay of insecticidal activity, Bm252RFP–Cry1A was synthesized with one molar Cry1A and two molar Bm252RFP, as an analogy to the above-mentioned reason to avoid the effects of insecticidal activity by unreacted Cry1A. The macrocomplex at various concentrations in 15 µl of 20 mM Tris-HCl buffer containing 50 mM NaCl, pH 8.0, was orally administered to each of the 10 1-day old fifth-instar silkworms; and mortality was recorded after 24 h. Bioassay was also done using Cry1A and P252-Cry1A. LD_{50} was obtained by probit analysis with a minimum of five independent assays (Russel et al. 1977). Neither P252 nor Bm252RFP had insecticidal activity (Pandian et al. 2008); hence, as mentioned above, activity of the macrocomplexes was expressed using the molar concentration of only Cry1A instead of Bm252RFP–Cry1A.

Western Blot Analysis of Bm252RFP–Cry1A

The completion of macrocomplex formation was evaluated with Western blot analysis of the synthesized Bm252RFP–Cry1A. The macrocomplexes synthesized were separated in 5% SDS gel and blotted on PVDF membranes as described in Hossain et al. (2004). Cry1Aa and Cry1Ab were detected with rabbit anti-Cry1Aa antiserum since the anti-Cry1Aa antiserum also can almost equally recognize Cry1Ab. Cry1Ac was detected with anti-Cry1Ac antiserum. Antibodies bound with toxin were visualized using peroxidase-conjugated goat anti-rabbit IgG (Amersham Pharmacia Biosciences, Piscataway, NJ) and ECL reagents (Amersham Pharmacia Biosciences) using a BAS-3000 detector (Fujifilm, Tokyo, Japan) as described in Hossain et al. (2004) and Pandian et al. (2008).

Absorption and Fluorescence Analysis of Bm252RFP–Cry1A

The absorption spectra of Bm252RFP–Cry1A in 1 ml of 20 mM Tris-HCl, pH 8.0, containing 50 mM NaCl were

monitored using a spectrophotometer with 500–700 nm wavelength. The fluorescence spectra were determined with a spectrofluorometer (RF5301; Shimadzu, Kyoto, Japan) by exciting with a wavelength of 495 nm at 25°C as shown in Pandian et al. (2008).

SDS and Native PAGE of Bm252RFP–Cry1A

SDS-PAGE and native PAGE were performed as described previously in Hossain et al. (2004) and in Kishimoto et al. (2001), respectively. The fluorescence of proteins was analyzed using LAS 3000 (Fujifilm) with wavelengths of 490 nm for excitation and 630 nm for emission.

Circular Dichroism Analysis of Bm252RFP and Bm252RFP–Cry1A

Far-UV circular dichroism (CD) analysis was performed using a spectropolarimeter (J-725; Jasco, Tokyo, Japan) with a 250-W xenon lamp. Cry1A and Bm252RFP were dissolved in 500 ml of 20 mM Tris-HCl containing 50 mM NaCl, pH 8.0, for 1.5 h at 25°C. The ratios of the concentration of Bm252RFP with Cry1Aa, Cry1Ab and Cry1Ac for the incubation were 1:1.7, 1:2.5 and 1:1.7, respectively. As described above, these ratios are almost optimal to make macrocomplexes from Bm252RFP and the respective Cry1As. Under these conditions, unreacted individual Bm252RFP and Cry1A were negligible, as will be shown in Figs. 1 and 2; thus, the CD spectra of each compound may not be affected by unreacted elements. Spectra were obtained and analyzed according to Yang et al. (1986) using the program SSE-338 (J-725, Jasco). The standard error was calculated from five independent experiments.

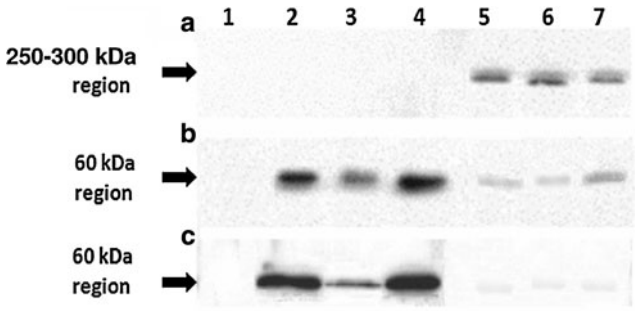

Fig. 2 Western blot analysis of Bm252RFP–Cry1A with anti-Cry1A antisera. Equimolar concentrations of Bm252RFP and respective Cry1As were reacted for 1.5 h and the reacted mixture was electrophoresed in 5% SDS gel. The proteins developed were blotted onto PVDF membranes, and Cry1A was detected with either anti-Cry1Aa or -Cry1Ac antiserum. Authentic Bm252RFP was shown at 250–300 kDa in lane 1 (**a**), and authentic Cry1Aa, Cry1Ab and Cry1Ac were shown at 60 kDa in lanes 2–4, respectively (**b**). Synthesized Bm252RFP–Cry1Aa, –Cry1Ab and –Cry1Ac were quantified with anti-Cry1Aa or -Cry1Ac antiserum in lanes 5–7 (**a**) at 250–300 kDa. Unreacted Cry1A in the reaction mixtures was visualized with the same antisera in lanes 5–7 (**b**). The reaction was also done with 1:2.4 molar concentration ratios of Bm252RFP and Cry1A and then, as mentioned, unreacted Cry1Aa, Cry1Ab and Cry1Ac were detected with the same antisera (**c**, lanes 5–7)

Protein Quantification

Various solubilized or chromatographed proteins were quantified with optical density at 280 nm or with the method of Bradford (1976). For CD analysis, the protein concentration was estimated by the Kjeldahl method (Shaw and Beadle 1949).

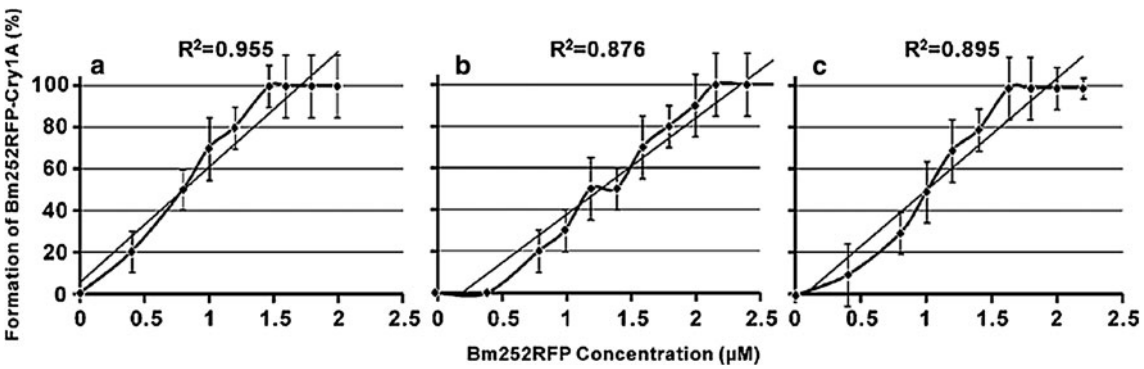

Fig. 1 Formation of Bm252RFP–Cry1A with Bm252RFP and Cry1A toxins. Cry1Aa, Cry1Ab and Cry1Ac toxins (1 μM each) were mixed with Bm252RFP at various concentrations (0.5–2.5 μM) at 25°C. Then, unbound Cry1A toxins were separated from synthesized Bm252RFP–Cry1A using size-exclusion chromatography and quantified with photo absorption at 280 nm. The amount of each Bm252RFP–Cry1A was plotted against the concentration of Bm252RFP used. For details, see "Materials and Methods" section

Results

Stoichiometry of Bm252RFP–Cry1A Formation

To establish the optimum condition for the formation of Bm252RFP–Cry1A macrocomplex, the stoichiometry of the reaction was explored by incubating Bm252RFP and Cry1A in various different ratios under aerobic/light conditions at room temperature (Fig. 1). The formation of complexes was monitored by separating Bm252RFP–Cry1A from unbound Cry1A toxins with size-exclusion chromatography equipped with GPC-1000 column, as mentioned in "Materials and Methods" section. For the complete synthesis of Bm252RFP–Cry1Aa, 1 μM Cry1Aa required 1.5 μM of Bm252RFP (Fig. 1a). To form Bm252RFP–Cry1Ab and Bm252RFP–Cry1Ac, the required Bm252RFP concentrations were 2.2 and 1.6 μM, respectively (Fig. 1b, c).

K_d values for the binding of Bm252RFP to Cry1Aa, Cry1Ab and Cry1Ac were calculated as described in Coleman and Pugh (1997) to be 79, 216 and 93 nM, respectively, from these reactions.

Western Blot Analysis to Check Completion of Bm252RFP–Cry1A Formation

Macrocomplex formation was also confirmed with Western blot analysis. Equimolar concentrations of Bm252RFP and Cry1A were incubated for 1.5 h under the same above-mentioned conditions, and the completion of macrocomplex synthesis was checked using Western blots. Before the synthetic reaction, all three authentic Cry1As were detected in the 60-kDa region (Fig. 2b, lanes 2–4) with their respective antisera, and Bm252RFP was detected at 250–300 kDa without any Cry1A signals (Fig. 2a, lanes 1–4). On the other hand, the reaction mixture showed clear signals of Cry1Aa, Cry1Ab and Cry1Ac at around 250–300 kDa (Fig. 2a, lanes 5–7). Though the optimal ratios between Cry1A and Bm252RFP for macrocomplex formation were different from each other as described in the stoichiometry of Bm252RFP–Cry1A formation, when incubated with a 1:1 concentration, we could expect a clear signal of Cry1A antisera at 250–300 kDa and possibly no signal from Cry1A toxins at 60 kDa, due to the formation Bm252RFP–Cry1A with a lower amount of Cry1A. As expected, a clear signal was shown at around 250–300 kDa but weak signals of Cry1A were also detected in the reaction mixture at 60 kDa (Fig. 2b, lanes 5–7). Although the reaction was carried out with equimolar concentrations of Bm252RFP and Cry1A, these thin signals corresponding to Cry1A must be derived from nonreacted Cry1A. Therefore, the ratio of concentration of Bm252RFP to Cry1A in the reaction mixture was increased to 1:2.4 to reduce the amount of any further nonreacted Cry1A toxins, and as expected, almost no signal was obtained in the 60-kDa region (Fig. 2c, lanes 5–7). However, a very weak signal in the 60-kDa region was always observed (Fig. 2c, lanes 5–7). These very thin signals could be interpreted either as the small amount of Cry1A that was released from the complex when subjected to SDS-PAGE or as that derived from nonreacted Cry1Aa. If the latter is the case, the concentration of Bm252RFP determined to be optimal in the stoichiometric analysis was slightly underestimated.

We used antiserum raised against P252 (Hossain et al. 2005) to distinguish the macromolecules from Bm252RFP in Western blots after SDS-PAGE, but determination of free Bm252RFP in the reaction mixture with the antiserum after the reaction was difficult as it was not easy to distinguish the 60-kDa molecular size even with a 5% gel. Nonetheless, all these data suggested that the optimal condition estimated to form Bm252RFP–Cry1A was reasonable and, if not, could not be far from those ratios shown in Fig. 1. These data guaranteed that the unreacted Cry1A or Bm252RFP had little or no effect on the bioassays for antimicrobial and insecticidal activities, which are shown later.

Influence of Various Parameters on the Stability of Bm252RFP–Cry1A

The stability of the complex of Bm252RFP–Cry1Aa, –Cry1Ab and –Cry1Ac under various conditions was determined by measuring the released Bm252RFP and/or Cry1A in 48-h incubation using Western blot analysis and gel filtration, as mentioned in "Materials and Methods" section. All three Bm252RFP–Cry1A macrocomplexes displayed almost the same tendencies during the stability studies. To avoid redundancy, here we only present the results of Bm252RFP–Cry1Ab due to its distinct binding characteristics, which will be discussed later.

The effect of pH was studied using Bm252RFP–Cry1A with various pH values from 6 to 11 as given in "Materials and Methods" section. A significant effect on the stability of Bm252RFP–Cry1Ab complexes was observed only after 24-h incubation with various pH values. Hence, the stability with 48-h incubation was analyzed, which indicated that the complex is most stable in the pH range of 8–10 (Fig. 3a). At pH 6–7, 40–50% of the Bm252RFP–Cry1Ab macrocomplex lost integrity by releasing Cry1Ab over 48 h, while at pH 10.5 only 20% of the macrocomplex lost integrity (Fig. 3a).

The effect of temperature on stability was studied at 25, 28, 30 and 37°C. At 25 and 28°C, Bm252RFP–Cry1Ab was stable for 12 h but lost its stability by about 25% with 48-h incubation (Fig. 3b). On the other hand, at 30 and 37°C, Bm252RFP–Cry1Ab lost stability by 25% over 12 h and lost 50% around 36 h, but further instability was not

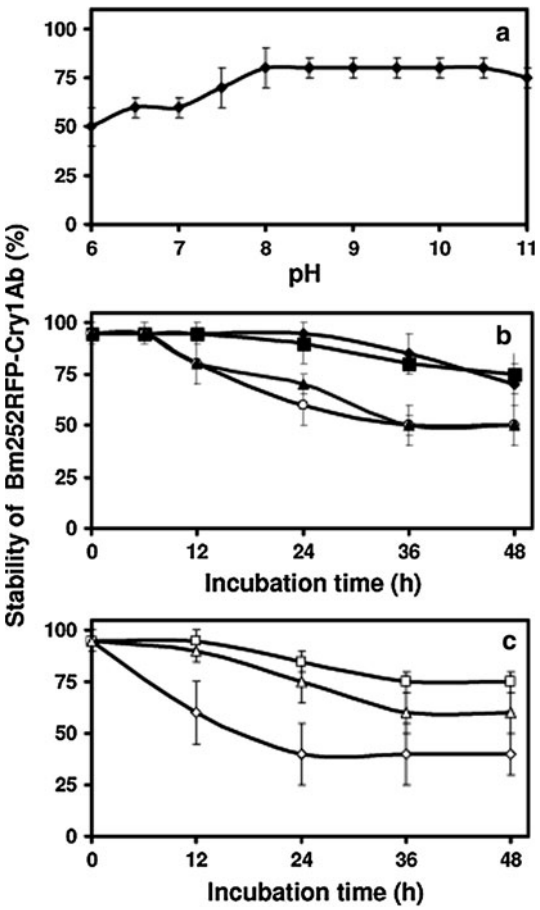

Fig. 3 Influence of parameters affecting the stability of Bm252RFP–Cry1Ab. Bm252RFP–Cry1Ab was incubated for 48 h, and its percent stability was calculated based on the release of Cry1A toxins and Chlide, analyzed by Western blotting, gel filtration and TLC as described in "Materials and Methods" section. To study the effect of pH, Bm252RFP–Cry1Ab was dissolved in corresponding buffer with various pH values (6–11) as mentioned in "Materials and Methods" section and the stability of the macrocomplex under these pH values after 48 h was estimated (**a**, *filled diamond*). To study the effect of temperature on the stability of Bm252RFP–Cry1Ab, the macrocomplex was dissolved in 20 mM Tris-HCl buffer containing 50 mM NaCl and the percent stability was measured every 12 h until 48 h (**b**; *filled square*, *filled diamond*, *open circle* and *filled triangle* correspond to 25, 28, 30 and 37°C, respectively). The effect of light on the stability of Bm252RFP–Cry1Ab was evaluated by measuring the release of Chlide every 12 or 48 h by incubating Bm252RFP–Cry1Ab in 20 mM Tris-HCl buffer containing 50 mM NaCl under dark conditions, low light conditions (4,132 $\mu molm^2\ s^{-1}$) and normal light conditions (6,000 $\mu molm^2\ s^{-1}$) represented by the symbols *open diamond*, *open square* and *open triangle*, respectively (**c**)

observed by prolonged incubation at these two temperatures (Fig. 3b).

Chlide was shown to be sensitive toward light intensity (Pandian et al. 2008), so the effect of light on the stability of the complex was determined using both TLC and Western blots. After 12-h incubation, about 95% of the complex retained stability under bright light with a photon flux density of 6,346 $\mu molm^{-2}\ s^{-1}$, while about 60% of the complex retained integrity with 48-h incubation (Fig. 3c); but the maximum stability of the complex was observed under low light conditions with a photon flux density of 4,132 $\mu molm^{-2}\ s^{-1}$, which retained 85 and 75% of integrity with 24- and 48-h incubation, respectively (Fig. 3c). However, in complete dark conditions, only about 60% and 40% of the complex was stable with 12- and 48-h incubation, respectively (Fig. 3c).

The stability of the complex was also checked under aerobic and anaerobic conditions with and without light. Maximum stability was obtained with the aerobic light condition at pH 8 and 25°C (data not shown). Therefore, based on all these data, the best conditions to maintain Bm252RFP–Cry1Ab with about 95% integrity for 12 h is to dissolve the complex in 20 mM Tris-HCl buffer at pH 8.0 and to incubate at 28°C under aerobic conditions in the presence of light with a photon flux density of 4,132 $\mu molm^2\ s^{-1}$.

It is important to note here that Bm252RFP–Cry1Ab was perfectly stable at 30 and 37°C until 7 h and the antimicrobial activity was measured with 4-h incubation. Furthermore, the other two macrocomplexes were also stable for the same period. These results again confirm that under the above optimal conditions all three macrocomplexes were stable during the assay of antimicrobial activity.

Antimicrobial Activity of Bm252RFP–Cry1A

EC_{50} values of Bm252RFP–Cry1A against various microbes were determined and are shown in Table 1. These values indicated that in the case of Bm252RFP–Cry1Ab the antimicrobial activity against the microbes used roughly retained the same respective EC_{50} value as that of Bm252RFP. However, in the case of Bm252RFP–Cry1Aa and Bm252RFP–Cry1Ac, about 30–35% of the activity was lost regardless of the microbes used.

Insecticidal Activity of Bm252RFP–Cry1A

The insecticidal activity of Bm252RFP–Cry1A was evaluated with an oral bioassay using 1-day-old fifth instar of *B. mori* larvae, and the mortality curve of the Bm252RFP–Cry1A macrocomplex is shown in Figure 4, with Cry1A and P252-Cry1A as control. LD_{50} values of Cry1Aa, Cry1Ab and Cry1Ac against *B. mori* larvae were determined to be 0.06, 1.6 and 134 µg/larva, respectively (Table 2). The P252–Cry1A complex did not show any significant reduction in the mortality of the corresponding Cry1A toxins. However, in the Bm252RFP–Cry1A complex, the mortality rate of only Bm252RFP–Cry1Ab was reduced by about three times while in the other two cases the complexes showed almost the same activity as that of the corresponding Cry1A toxins.

Table 1 Antimicrobial activity of Bm252RFP and Bm252RFP–Cry1Aa toxins

Microbes	EC_{50} concentration (μM)			
	Bm252RFP	Bm252RFP–Cry1Aa	Bm252RFP–Cry1Ab	Bm252RFP–Cry1Ac
E. coli	2.8 ± 0.1	3.9 ± 0.3	2.8 ± 0.3	4.0 ± 0.3
Se. marcescens	2.9 ± 0.2	4.2 ± 0.2	3.3 ± 0.4	4.5 ± 0.4
B. thuringiensis	6.0 ± 0.8	7.9 ± 0.9	6.4 ± 0.8	7.9 ± 0.7
Sa. cerevisiae	21.6 ± 1.2	31.8 ± 2.2	26.1 ± 1.4	32.6 ± 1.9

Bm252RFP, Bm252RFP–Cry1Aa, –Cry1Ab and –Cry1Ac complexes in various concentrations were added to each microbial culture suspension and EC_{50} concentrations, showing 50% growth inhibitory effect against microbes, were evaluated. SEM was calculated based on six independent experiments

Comparison of Emission of Red Fluorescence and Photo Absorption among Bm252RFP–Cry1A

All of the above data suggested that the characteristics of the Bm252RFP–Cry1Ab complex were different from those of the other two macrocomplexes. Therefore, we compared the characteristic photo absorption and fluorescence emission among Bm252RFP–Cry1A synthesized with a 1:2.4 molar concentration between Cry1A and Bm252RFP. With this ratio, all Bm252RFP was expected to alter to Bm252RFP–Cry1A (Fig. 1). The complexes were applied to native PAGE to visualize the red fluorescence emitted. Since the red fluorescence is derived from Bm252RFP, all Bm252RFP–Cry1A were expected to have the same intensity as that of Bm252RFP, even in Bm252RFP–Cry1Ab (Pandian et al. 2008). Contrary to our expectation, interestingly, the red fluorescence intensity of Bm252RFP–Cry1Ab was significantly reduced compared to that of the other two macrocomplexes (Fig. 5a). We quantitatively estimated the absorbance and fluorescence emission spectra of those complexes. Bm252RFP–Cry1Aa and Bm252RFP–Cry1Ac were shown to have identical intensities in the fluorescence spectra at 620 nm, but Bm252RFP–Cry1Ab showed a substantially low intensity in the fluorescence emission (Fig. 5b). Photo absorption of these three macrocomplexes was also different, and the absorption at 600 nm in Bm252RFP–Cry1Ab was significantly lower than that of the other two macrocomplexes (Fig. 5c).

Table 2 LD_{50} values of Cry1A, P252–CrylAa and Bm252RFP–Cry1Aa

Samples	LD_{50} (jag/larva) (95% confidence interval)
CrylAa	0.06 (0.04–0.8)
P252–CrylAa	0.06 (0.04–0.8)
Bm252RFP–Cry1Aa	0.07 (0.05–0.8)
CrylAb	1.6 (1.2–2.0)
P252–CrylAb	1.8 (1.2–2.0)
Bm252RFP–CrylAb	5.1 (1.2–6.0)
Cry1Ac	134 (121–190)
P252–CrylAc	147 (123–192)
Bm252RFP–CrylAc	143 (124–190)

Cry1Aa, Cry1Ab, Cry1Ac and their complexes with either P252 or Bm252RFP were adjusted to various concentrations and given to 10 1-day-old fifth-instar larvae of *Bombyx mori* to determine the LD_{50} as described in "Materials and Methods"

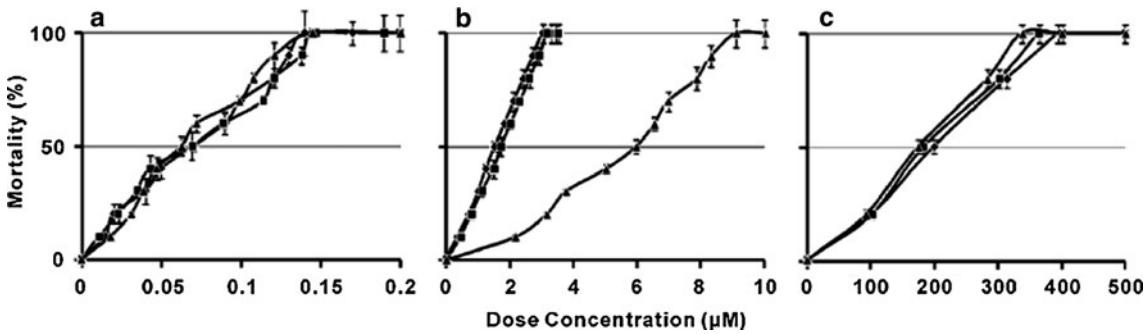

Fig. 4 Mortality curve of *B. mori* larvae with Cry1A, P252-Cry1A and Bm252RFP–Cry1A. Ten 1-day-old fifth-instar larvae of *B. mori* were fed with various complexes related to Cry1Aa (**a**), Cry1Ab (**b**) and Cry1Ac (**c**) at various concentrations. In each panel, the symbols *filled triangle*, *filled square* and *filled diamond* represents Cry1A, P252-Cry1A and Bm252RFP–Cry1A, respectively. Mortality was expressed as a percentage of the activity of the compounds with Cry1Aa, Cry1Ab and Cry1Ac

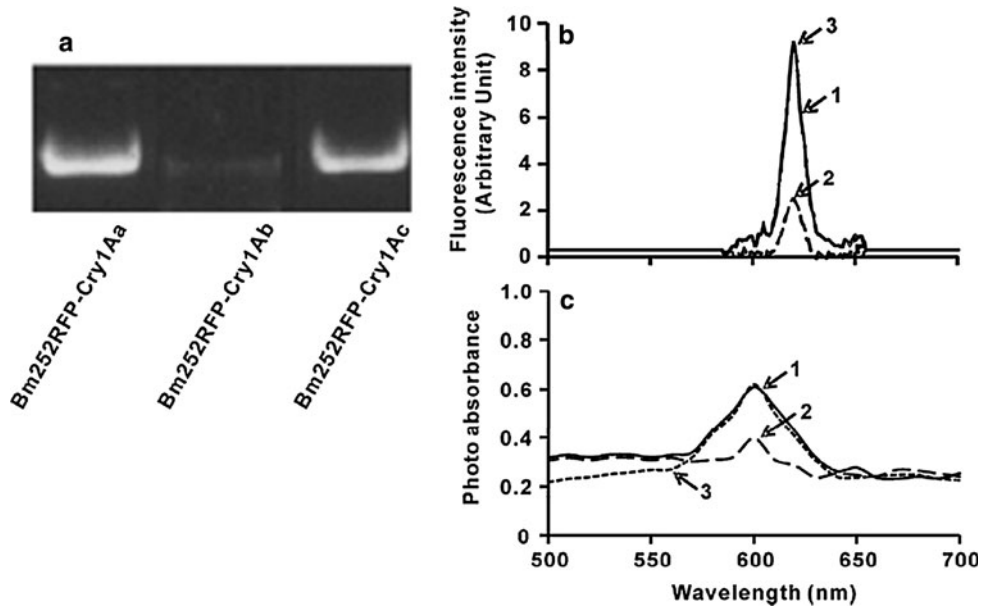

Fig. 5 Red fluorescence, photo absorption and fluorescence spectra of Bm252RFP–Cry1A. **a** Each Bm252RFP–Cry1A (1 μM) was applied to native PAGE with 5% gel and fluorescence was analyzed using LAS 3000 at 630 nm emission. **b** The fluorescence intensity of 1 μM of each macrocomplex was checked at 25°C using a spectrofluorometer with excitation and emission wavelengths at 495 and 620 nm, respectively. **c** Photo absorption spectra with wavelengths from 500 to 700 nm were measured using a UV-Vis spectrophotometer. All samples were suspended in a total volume of 1 ml of 20 mM Tris-HCl, pH 8.0, containing 50 mM NaCl. Lines 1–3 represent Bm252RFP–Cry1Aa, –Cry1Ab and –Cry1Ac, respectively

Comparison of CD Spectra of Cry1A, Bm252RFP and Bm252RFP–Cry1A

The above results suggested that the structure of Bm252RFP–Cry1Ab was different from that of Bm252RFP–Cry1Aa and –Cry1Ac in Bm252RFP and/or in Cry1A. In previous experiments, P252 was shown to have a large amount of β-structure but fewer α-helices (Pandian et al. 2008). Therefore, it is interesting to check the change in the α-helical structure of Bm252RFP–Cry1Ab to interpret the reduction in the above-mentioned photo absorption and fluorescence emission. To investigate the change in secondary structure, CD spectra were measured as mentioned in "Materials and Methods" section (Fig. 6), and Bm252RFP was shown to contain mainly β-structure (21.6 ± 3.1%), other conformations (75.3 ± 2.9%) and almost no α-helices (Fig. 6a–c). Three Cry1As were shown to have an average of about 29.0 ± 1.5% of α-helices along with 22.4 ± 3.4% of β-structure and other conformations (63 ± 5.1%) (Fig. 6a–c). On binding with Bm252RFP, the α-helix of Cry1Ab was significantly reduced from 27.4 ± 1.6% to 12.6 ± 2.2% (Fig. 6b). On the other hand, in Cry1Aa and Cry1Ac, the respective α-helical contents of 28.9 ± 2.4% and 27.8 ± 1.3% were only slightly reduced to 25.6 ± 1.7% and 23.9 ± 0.9%, respectively, after binding with Bm252RFP (Fig. 6a, c). Since Bm252RFP had almost no α-helical structure, this reduction of α-helix in the Bm252RFP–Cry1Ab complex should have been derived from conformational change of the α-helical structure in Cry1Ab. As mentioned above (also see Fig. 6), although the change in β-structure of Bm252RFP and Bm252RFP–Cry1Ab wa shown, unfortunately, it was not clear which part of the macrocomplex was responsible for this reduction. We also analyzed CD spectra on the formation of P252–Cry1Aa, –Cry1Ab and –Cry1Ac. Interestingly, the CD spectra of P252–Cry1Ab and P252–Cry1Ac did not show any significant change with binding and only a weak change was observed with binding of P252 and Cry1Aa (data not shown).

Discussion

Binding of Chlorophyllide with 252-kDa *Bombyx mori* Midgut Protein

The insecticidal mechanism of Bt Cry toxins has not yet been fully elucidated. Nevertheless, it is generally accepted that a receptor protein(s) interacts with the toxins, leading to pore formation in the midgut cell membrane of the susceptible insect larvae.

P252 was isolated from *B. mori* midgut epithelial cells, and binding to Cry1A toxins with K_d of 29, 280 and 20 nM for Cry1Aa, Cry1Ab and Cry1Ac, respectively, was shown (Hossain et al. 2004); recently, P252 was also shown to bind with chlorophyllide to form the red fluorescence–emitting

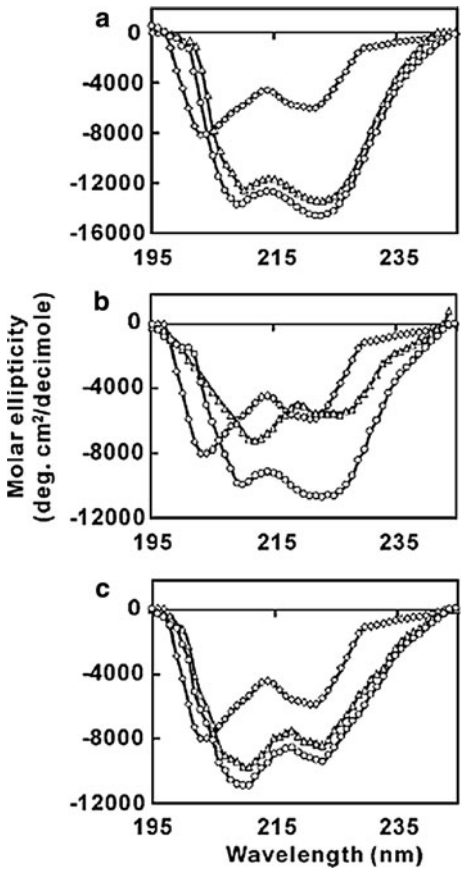

Fig. 6 CD spectra of Cry1A, Bm252RFP and Bm252RFP–Cry1A. Purified Cry1A toxins, Bm252RFP and Bm252RFP–Cry1A were individually dissolved in 500 µl of 20 mM Tris-HCl, pH 8.0, containing 50 mM NaCl and subjected to CD analysis. **a** Secondary structure of Cry1Aa, Bm252RFP–Cry1Aa and Bm252RFP used in this study. **b** Secondary structure of Cry1Ab, Bm252RFP–Cry1Ab and Bm252RFP. **c** Secondary structure of Cry1Ac, Bm252RFP–Cry1Ac and Bm252RFP. The complexes subjected to analysis are represented with the symbols *open circle*, *open diamond* and *open triangle* for Cry1A, Bm252RFP and Bm252RFP–Cry1A, respectively. For details, see "Materials and Methods" section

protein complex, termed "Bm252RFP" (Pandian et al. 2008). Although the binding of P252 to Cry1A toxins was strong in affinity, its real roles in insecticidal activity have not been elucidated. In addition, Bm252RFP has been shown to have strong antimicrobial activity against various microbes. Here, we examined the binding capability of Bm252RFP to Cry1A toxins and investigated the effect of its binding on the antibacterial and insecticidal activities to explore the unknown physiological role(s) of P252.

Formation of Bm252RFP–Cry1A

Bm252RFP was clearly shown to form the macrocomplex Bm252RFP–Cry1A with all three Cry1As. In order to form these complexes, 1 µM of Cry1Aa, Cry1Ab and Cry1Ac required 1.5, 2.2 and 1.6 µM of Bm252RFP, respectively. The K_d values of the binding of those three toxins to Bm252RFP were 79, 216 and 93 nM, respectively, which were roughly the same as those of formation of P252–Cry1A complexes, as mentioned above (Hossain et al. 2004). Interestingly, the macrocomplex was most stable in an alkaline pH of 8–10 and not in an acidic or neutral pH of 6–7.5; it must be noted that the pH of the insect midgut fluid is generally in the range 8–11. Bm252RFP–Cry1A was also stable under low light conditions with a photon flux density of 4,132 µmol/m^2/s but not at normal room light conditions of 6,346 µmol/m^2/s. It is important to note here that with alkaline pH and low light conditions like in the midgut of *B. mori*, at least about 50% of the complexes were stable, depending on the temperature, for 48 h. At this moment, none of the physiological roles of Bm252RFP–Cry1A is clear, but these physicochemical characteristics must be important to elucidate the roles of the complex in vivo in our future studies. In our study, we observed that when *B. mori* was reared with an artificial diet, which contains only a trace of chlorophyllide, P252 displayed only weak fluorescence. However, when we reared *B. mori* in mulberry leaves, P252 gained significant red fluorescence (data not shown). This result strongly suggested the existence of Bm252RFP in *B. mori* under natural field conditions and supports the possibility of forming a macrocomplex with Cry1A.

Antimicrobial Activity of Bm252RFP–Cry1A

Bm252RFP–Cry1Aa and –Cry1Ac were shown to reduce antimicrobial activity. However, they retained about 70% activity of the Bm252RFP alone, regardless of the microbes used; and this reduced activity was still physiologically sufficient (Table 2). On the other hand, though the antimicrobial activity of Bm252RFP–Cry1Ab was also reduced, the reduction was the least among the three complexes and it retained about 80–90% of the activity of Bm252RFP (Table 2). Interestingly, the antimicrobial activity of Bm252RFP was relatively stable in the larval midgut juice of *B. mori* for about 12 h (Pandian et al. unpublished data). This observation suggests the possibility that Bm252RFP–Cry1A also plays a role in antimicrobial immunity in insect midgut and that the macrocomplex is bifunctional.

As shown in Fig. 6, the secondary structure of Cry1A molecules was changed when they formed Bm252RFP–Cry1A; but different from the reduction of insecticidal activity, it is not straightforward to explain the reduction in antimicrobial activity in the macrocomplex with an altered secondary structure as at this moment the real mechanism of the antimicrobial activity is not known. As will be briefly discussed later, radical formation could be involved

in this activity and change in secondary structure could affect the radical generation.

Insecticidal Activity of Bm252RFP–Cry1A

Bm252RFP–Cry1A was shown to have insecticidal activity, and only the mortality curve of Bm252RFP–Cry1Ab was affected; the LD_{50} of Cry1Ab was shown to increase by three times (Fig. 4b). However, in the cases of Cry1Aa and Cry1Ac, their insecticidal activities were retained in P252–Cry1Aa and –Cry1Ac and in Bm252RFP–Cry1Aa and –Cry1Ac, respectively (Fig. 4a, c). The LC_{50} of Cry1Ab against *B. mori,* hybrid Shunrei × Shogetsu, is 8.13 μg toxin/g diet and those of Cry1Aa and Cry1Ac are 0.23 and >734 μg, respectively (Shitomi et al. 2006). This strain was very sensitive toward Cry1Aa but tolerant to Cry1Ab by 35 times and Cry1Ac by 3,200 times compared to the susceptibility toward Cry1Aa. If the binding of Cry1Ab to Bm252RFP takes place in the *B. mori* larval midgut, it may reduce the insecticidal activity and bring in part the tolerance of *B. mori* larvae against Cry1Ab. On the other hand, Cry1Ac did not change its insecticidal activity upon macrocomplex formation; therefore, though *B. mori*, hybrid Shunrei × Shogetsu, is significantly tolerant to Cry1Ac, the macromolecule obviously does not play any role in the tolerance.

The reduction of insecticidal activity on the formation of Bm252RFP–Cry1Ab was the most significant compared to the other two macrocomplexes. It is interesting to speculate on why only Cry1Ab reduces the insecticidal activity in Bm252RFP–Cry1Ab. In this aspect, the α-helical structure is important since the α-helix in domain I is thought to be the part that penetrates into the plasma membrane (Bravo et al. 2005; Tomimoto et al. 2006; Tapaneeyakorn et al. 2005; Nair and Dean 2008); therefore, the pore formation seems to depend on the length and amount of the α-helices. The α-helical structure of Cry1Aa and Cry1Ac was not changed on binding with Bm252RFP, but the content in Cry1Ab was significantly reduced on binding with Bm252RFP (Fig. 6). Although the fashion of conformational change of Cry1Ab in the Bm252RFP–Cry1Ab complex is not clear in detail, as mentioned above, it may be involved in the reduction of insecticidal activity. Reduction of α-helical contents in Bm252RFP–Cry1Ab is suggested to partially abort the penetration of the α-helices in Bm252RFP–Cry1Ab into the plasma membrane. Thus, formation of the macrocomplex with Cry1Ab toxin is suggested to play some role in insect tolerance against Cry1Ab. Although the physiological role(s) of P252 needs more clarification, it is interesting to point out that in the studies with antiserum raised against *B. mori* P252, a large-sized (200–300 kDa) protein positive to the antiserum was found in BBMVs prepared from *Aedes aegypti* mosquito larvae (Moonsom 2007, PhD thesis, Mahidol University, Thailand). If this is the case in many other insects, it may be implied that the 252-kDa protein, as well as other RFPs, could be a common protein in antimicrobial systems in insects.

Lipocalin Family and Red Fluorescent Protein

Internal peptides of P252 are shown to have sequence similarity to lipocalin (Mauchamp et al. 2006; Pandian et al. 2008). A protein belonging to the lipocalin family, lipocalin-2, is known to play an important role as an innate immune protein to sequester iron from bacteria (Flo et al. 2004; Ong et al. 2006). Whether the macrocomplex Bm/lipocalin/RFP also plays some role in the insect immunity by providing antimicrobial activity, even if it does not typically function as lipocalin, remains to be studied. In addition, polycalin with aminopeptidase activity has been shown to be present in *Helicoverpa armigera* larvae (Angelucci et al. 2008); therefore, if this has binding capability with Chlide and Cry1As, a certain lipocalin with aminopeptidase activity must be the key protein(s) to regulate tolerance to Cry1As and microbes via the formation of various macrocomplexes. The physiological roles of the macrocomplex should be elucidated for the long-lasting use of environment-friendly insecticides and for understanding the physiological aspects of the insect midgut.

It is important to answer the newly raised question, How does the innate immune system distinguish invading nonprofitable bacteria from symbiotic good ones? From our preliminary experiments using scavengers, radical formation has been thought to be a reason for the antimicrobial activity (data not shown). Thus, the invading nonprofitable bacteria must be different from each other in sensitivity to those radicals and the beneficial bacteria survive. From an alternative view, only bacteria that are tolerant to the signaling of this radical to avoid oxidative stress can live close together in the insect midgut.

Acknowledgments This work was supported, in part, by research grants from the Ministry of Education, Culture, Sports, Science and Technology (13306006 and 12558069 to H. H.) and a grant for the promotion of the Niigata University Research Project (2004) (also to H. H.). We also thank the student scholarships awarded to G. P. by the Ministry of Education, Culture, Sports, Science and Technology. C. A. visited H. H.'s laboratory to discuss this research in the short-range exchange program for foreign researchers of Japan Society for the Promotion of Science (S-08207).

References

Angelucci C, Aarrett-Wilt BG, Hunt DF, Akhurst RJ, East PD, Gordon KH, Campbell PM (2008) Diversity of aminopeptidases, derived from four lepidopteran gene duplications, and polycalins expressed in the midgut of *Helicoverpa armigera*: identification

of proteins binding the delta-endotoxin, Cry1Ac of *Bacillus thuringiensis*. Insect Biochem Mol Biol 38:685–696

Bergman P, Johansson L, Wan H, Jones A, Gallo RL, Gudmundsson GH, Hökfelt T, Jonsson AB, Agerberth B (2006) Induction of the antimicrobial peptide CRAMP in the blood–brain barrier and meninges after meningococcal infection. Infect Immun 74:6982–6991

Bradford MM (1976) A rapid and sensitive method for the quantitation of microgram quantities of protein utilizing the principle of protein-dye binding. Anal Biochem 72:248–254

Bravo A, Soberón M, Gill SS (2005) *Bacillus thuringiensis*: mechanisms and use. In: Gilbert LI, Iatrou K, Gill SS (eds) Comprehensive molecular insect science, vol 6. Elsevier, Amsterdam, pp 175–205

Bravo A, Gill SS, Soberón M (2007) Mode of action of *Bacillus thuringiensis* Cry and Cyt toxins and their potential for insect control. Toxicon 49:423–435

Coleman RA, Pugh BF (1997) Slow dimer dissociation of the TATA binding protein dictates the kinetics of DNA binding. Proc Natl Acad Sci USA 94:7221–7226

Federici B (2003) Effects of Bt on non-target organisms. In: Metz M (ed) *Bacillus thuringiensis*: a cornerstone of modern agriculture. Food Products Press, Binghamton, NY, pp 11–30

Ferré J, Van Rie J (2002) Biochemistry and genetics of insect resistance to *Bacillus thuringiensis*. Annu Rev Entomol 47:501–533

Flo TH, Smith KD, Sato S, Rodriguez DJ, Holmes MA, Strong RK, Akira S, Aderem A (2004) Lipocalin 2 mediates an innate immune response to bacterial infection by sequestrating iron. Nature 432:917–921

Gill SS, Cowles EA, Francis V (1995) Identification, isolation, and cloning of a *Bacillus thuringiensis* CryIAc toxin-binding protein from the midgut of the lepidopteran insect *Heliothis virescens*. J Biol Chem 270:27277–27282

Griffitts JS, Aroian RV (2005) Many roads to resistance: how invertebrates adapt to Bt toxins. Bioessays 27:614–624

Heckel DG (1994) The complex genetic basis of resistance to *Bacillus thuringiensis* toxin in insects. Biocontrol Sci Technol 4:405–417

Hossain DM, Shitomi Y, Hayakawa T, Higuchi M, Mitsui T, Sato R, Hori H (2004) Characterization of a novel plasma membrane protein, expressed in the midgut epithelia of *Bombyx mori* that binds to Cry1A toxins. Appl Environ Microbiol 70:4604–4612

Hossain DM, Shitomi Y, Nanjo Y, Takano D, Nishiumi T, Hayakawa T, Mitsui T, Sato R, Hori H (2005) Localization of a novel 252-kDa plasma membrane protein that binds Cry1A toxins in the midgut epithelia of *Bombyx mori*. Appl Entomol Zool 40:125–135

Ihara H, Uemura T, Masuhara M, Ikawa S, Sugimoto S, Wadano A, Himeno M (1998) Purification and partial amino acid sequences of the binding protein from *Bombyx mori* for CryIAa δ-endotoxin of *Bacillus thuringiensis*. Comp Biochem Physiol B 120:197–204

Indrasith LS, Ogiwara K, Minami M, Iwasa T, Maruyama T, Suzuki N, Asano S, Sakanaka K, Hori H (1991) Processing of delta endotoxin from *Bacillus thuringiensis* subspp. *Kurstaki* HD-1 and HD-73 by immobilized trypsin and chymotrypsin. Appl Entomol Zool 26:485–492

Janmaat AF, Myers J (2003) Rapid evolution and the cost of resistance to *Bacillus thuringiensis* in greenhouse populations of cabbage loopers, *Trichoplusia ni*. Proc R Soc Lond B Biol Sci 270:2263–2270

Kim YS, Kanda K, Kato F, Murata A (1998) Effect of the carboxyl terminal portion of Cry1Ab in *Bacillus thuringiensis* on toxicity against the silkworm, *Bombyx mori*. Appl Entomol Zool 33:473–477

Kishimoto T, Hori H, Takano D, Nakano Y, Watanabe M, Mitsui T (2001) Rice α-mannosidase digesting the high mannose glycopeptide of glutelin. Physiol Plant 112:15–24

Knight PJ, Crickmore N, Ellar DJ (1994) The receptor for *Bacillus thuringiensis* Cry1A(c) δ-endotoxin in the brush border membrane of the lepidopteran *Manduca sexta* is aminopeptidase N. Mol Microbiol 11:429–436

Kough J (2003) The safety of *Bacillus thuringiensis* for human consumption. In: Metz M (ed) *Bacillus thuringiensis*: a cornerstone of modern agriculture. Food Products Press, Binghamton, NY, pp 1–10

Mauchamp B, Royer C, Garel A, Jalabert A, Rocha MD, Grenier AM, Labas V, Vinh J, Mita K, Kadono K, Chavancy G (2006) Polycalin (chlorophyllide A binding protein), a novel, very large fluorescent lipocalin from the midgut of the domestic silkworm *Bombyx mori* L. Insect Biochem Mol Biol 36:623–633

Moonsom S (2007) Characterization of *Bacillus thuringiensis* Cry4Ba -Binding proteins from midgut epithelium and peritrophic membrane of *Aedes aegypti* larvae. PhD thesis, Mahidol University, Thailand.

Nagamatsu Y, Toda S, Koike T, Miyoshi Y, Shigematsu S, Kogure M (1998) Cloning, sequencing, and expression of the *Bombyx mori* receptor for *Bacillus thuringiensis* insecticidal CryIA (a) toxin. Biosci Biotechnol Biochem 62:727–734

Nair MS, Dean DH (2008) All domains of Cry1A toxins insert into insect brush border membranes. J Biol Chem 283:26324–26331

Ong ST, Ho JZ, Ho B, Ding JL (2006) Iron-withholding strategy in innate immunity. Immunobiology 211:295–314

Pandian NG, Ishikawa T, Togashi M, Shitomi Y, Haginoya K, Yamamoto K, Nishiumi T, Hori H (2008) *Bombyx mori* midgut membrane protein P252 which binds to Cry1A of *Bacillus thuringiensis* is a chlorophyllide binding protein and its resulting complex has antimicrobial activity. Appl Environ Microbiol 74:1324–1331

Pigott CR, Ellar DJ (2007) Role of receptors in *Bacillus thuringiensis* crystal toxin activity. Microbiol Mol Biol Rev 71:255–281

Russel RM, Robertson JL, Savin NE (1977) POLO: a new computer program for probit analysis. Bull Entomol Soc Am 23:209–213

Sangadala S, Walters FS, English LH, Adang MJ (1994) A mixture of *Manduca sexta* aminopeptidase and phosphatase enhances *Bacillus thuringiensis* insecticidal CryIA(c) toxin binding and $^{86}Rb^{+}$-K^{+} efflux in vitro. J Biol Chem 269:10088–10092

Schnepf E, Crickmore N, Van Rie J, Lereclus D, Baum J, Feitelson J, Zeigler DR, Dean DH (1998) *Bacillus thuringiensis* and its pesticidal crystal proteins. Microbiol Mol Biol Rev 62:775–806

Shaw J, Beadle LC (1949) A simplified ultra-micro Kjeldahl method for the estimation of protein and total nitrogen in fluid samples of less than 1.0 µl. J Exp Biol 26:15–23

Shelton AM, Roberson JL, Tang JD, Perez C, Eigenbrode SD, Preisler HK, Wilsey WK, Cooley RJ (1993) Resistance of diamondback moth (*Lepidoptera: Plutellidae*) to *Bacillus thuringiensis* subspecies in the field. J Econ Entomol 8:697–705

Shitomi Y, Hayakawa T, Hossain DM, Higuchi M, Miyamoto K, Nakanishi K, Sato R, Hori H (2006) A novel 96-kDa aminopeptidase localized on epithelial cell membranes of *Bombyx mori* midgut, which binds to Cry1Ac toxin of *Bacillus thuringiensis*. J Biochem 139:223–233

Suzuki M, Hori H, Ogiwara K, Asano S, Sato R, Ohba M, Iwahana H (1992) Insecticidal spectrum of a novel isolate of *Bacillus thuringiensis* serovar japonensis. Biol Control 2:138–142

Tabashnik BE (1994) Evolution of resistance to *Bacillus thuringiensis*. Annu Rev Entomol 39:47–79

Tapaneeyakorn S, Pornwiroon W, Katzenmeier G, Angsuthanasombat C (2005) Structural requirements of the unique disulphide bond and the proline-rich motif within the α4–α5 loop for larvicidal

activity of the *Bacillus thuringiensis* Cry4Aa δ-endotoxin. Biochem Biophys Res Commun 330:519–525

Tomimoto K, Hayakawa T, Hori H (2006) Pronase digestion of brush border membrane-bound Cry1Aa shows that almost the whole activated Cry1Aa molecule penetrates into the membrane. Comp Biochem Physiol B 144:413–422

Vadlamudi RK, Weber E, Ji I, Ji TH, Bulla LA Jr (1995) Cloning and expression of a receptor for an insecticidal toxin of *Bacillus thuringiensis*. J Biol Chem 270:5490–5494

Valaitis AP, Lee MK, Rajamohan F, Dean DH (1995) Brush border membrane aminopeptidase-N in the midgut of the gypsy moth serves as the receptor for the CryIA(c) δ-endotoxin of *Bacillus thuringiensis*. Insect Biochem Mol Biol 25:1143–1151

Van Rie J, McGaughey WH, Johnson DE, Barnett BD, Van Mellaert H (1990) Mechanism of insect resistance to the microbial insecticide *Bacillus thuringiensis*. Science 247:72–74

Yang JT, Wu CS, Martinez HM (1986) Calculation of protein conformation from circular dichroism. Methods Enzymol 130:208–269